Water Research 169 (2020) 115225

Contents lists available at ScienceDirect

Water Research

journal homepage: www.elsevier.com/locate/watres

Rapid changes in organochlorine pesticides in sediments from the East China sea and their response to human-induced catchment changes

Chenglong Wang [a], Zhe Hao [b, c, *], Ziyue Feng [a], Chuchu Zhang [a], Jianhua Gao [a], Yali Li [a, c], Wenwen Yu [a, d], Xinqing Zou [a, c, **]

[a] School of Geographic and Oceanographic Sciences, Ministry of Education Key Laboratory for Coast and Island Development, Nanjing University, Nanjing, 210093, China
[b] Key Laboratory of Engineering Oceanography, Second Institute of Oceanography, Ministry of Natural Resources, Hangzhou, 310012, China
[c] Collaborative Innovation Center of South China Sea Studies, Nanjing University, Nanjing, 210093, China
[d] Marine Fisheries Research Institute of Jiangsu Province, Nantong, 226007, China

ARTICLE INFO

Article history:
Received 26 June 2019
Received in revised form
22 October 2019
Accepted 23 October 2019
Available online 24 October 2019

Keywords:
Organochlorine pesticides
Sediment grain size
Human activity
Catchment changes
Three gorges dam
East China sea

ABSTRACT

Human-induced catchment changes have affected the sedimentary processes in marginal seas, which will impact the transport and burial processes of materials and inevitably impact marine biogeochemical cycles. Organochlorine pesticides (OCPs) and sediment characteristics in surface sediments from the East China Sea (ECS) at two time points (2006 and 2018) were compared to understand the response of OCPs to human-induced catchment changes. A significant coarsening trend occurred after the impoundment of the Three Gorges Dam (TGD), with the mean grain size increasing from 6.4 ± 1.2 Φ to 4.4 ± 2.1 Φ, suggesting that the sedimentary environment in the ECS changed drastically. OCP concentrations in the ECS evidently decreased after the impoundment of the TGD, with mean values decreasing from 2.55 ± 1.51 ng g^{-1} to 1.08 ± 0.84 ng g^{-1}. The deposition flux of OCP also decreased from 2.65 ± 1.67 ng cm^{-2} yr^{-1} to 0.89 ± 0.60 ng cm^{-2} yr^{-1}. The reduction in the riverine input might be the reason that caused variations in the OCP concentration and deposition flux. In addition, sediment coarsening is likely to be the another primary factor influencing the differences in the distribution and deposition flux of the OCPs in the ECS. Therefore, the distribution and burial of OCPs in the ECS have been changed drastically, which may broadly impact the marine environment and biogeochemical cycles.

1. Introduction

Anthropogenic threats, such as pollution, that affect the oceans since the beginning of the Anthropocene are unprecedented (Steffen et al., 2007; Lewis and Maslin, 2015). These threats are altering the physicochemical properties and health of the world's oceans and influencing the survival of marine organisms (Alava et al., 2017). Since the 20th century, large amounts of synthetic compounds have been invented and used worldwide, including organochlorine pesticides (OCPs), which have been used extensively since the 1940s. Their concentrations in the environment have increased gradually and peaked during 1970–1990 (Li and Macdonald, 2005). Although these OCPs have been restricted or banned in most countries several decades ago, they can still be detected in various environmental compartments such as air, water, soil, sediment, and ice (Lewalle et al., 2009; Wong et al., 2012; Li et al., 2017; Jin et al., 2017; Bigot et al., 2017). These OCPs eventually enter marine environments through atmospheric deposition and surface runoff (Yang et al., 2005; Hu et al., 2011; Lin et al., 2015), resulting in marginal seas (a marginal sea is located at the edge of the continent, separated from the ocean by a peninsula, island, or archipelago, and connected to the ocean only by a strait or channel) being recognized as important sinks of OCPs (Guan et al., 2009; Hu et al., 2011; Ali et al., 2014). Therefore, much attention has been paid to coastal oceans owing to the accumulation of OCPs because they are recognized to have adverse effects on marine organisms and even the surrounding residents (Connor et al., 2007; Greenfield et al., 2015).

Estuarine–inner shelf areas are important components of

* Corresponding author. Key Laboratory of Engineering Oceanography, Second Institute of Oceanography, Ministry of Natural Resources, Hangzhou, 310012, China.
** Corresponding author. School of Geographic and Oceanographic Sciences, Ministry of Education Key Laboratory for Coast and Island Development, Nanjing University, Nanjing, 210093, China.
E-mail addresses: fishhaozhe@163.com (Z. Hao), zouxq@nju.edu.cn (X. Zou).

https://doi.org/10.1016/j.watres.2019.115225
0043-1354/

coastal oceans as they receive large amounts of terrestrial materials discharged via riverine inputs (Gao and Collins, 2014). However, the transport of terrestrial materials from river catchments to estuaries has decreased substantially owing to intensive human activities in river catchments (e.g., dam construction, land use change, and water withdrawal) (Syvitski et al., 2005; Milliman and Farnsworth, 2013), which have modified the sedimentary environment and ecosystems in the estuarine shelf regions (Gao, 2013; Gao et al., 2017, 2019; Yang et al., 2018). OCP loads associated with sediment loads are also likely to have decreased significantly, resulting in a changed flux to the ocean. Thus, human activities have modified the source-to-sink transport process of terrestrial materials, which in turn has influenced the transmission of OCPs in river catchment–estuary–shelf systems. Accordingly, it is necessary to investigate the impact of human-induced catchment changes on the source-to-sink transport mechanisms of OCPs in coastal oceans.

The East China Sea (ECS) is a typical marginal sea dominated by the Changjiang (Yangtze) River, which is facing severe pressure from human activities. Terrestrial input and atmospheric deposition have resulted in large amounts of OCPs entering the ECS, making this region an important OCP sink (Hu et al., 2011; Lin et al., 2012, 2013). However, the official ban on OCP use has been in force for several decades, causing a decreasing trend for dichlorodiphenyltrichloroethane (DDT) and hexachlorocyclohexane (HCH) levels in the air (Zhang et al., 2002; Lin et al., 2012), and even leading to the secondary release of OCPs from the ECS (Lin et al., 2015; Li et al., 2017). Due to human activities (especially dam construction), the transport of terrestrial materials from river catchments to the ECS has also substantially changed (Gao et al., 2018; Yang et al., 2018). More than 50,000 reservoirs have been constructed in the Changjiang (Yangtze) River catchment (Yang et al., 2011), which intercept sediments at a rate of 453 Mt yr^{-1} (million tons per year) (Gao et al., 2018). Sediment discharge has decreased steadily from 511 Mt yr^{-1} in 1956–1968 to 450 Mt yr^{-1} in 1969–1985, 340 Mt yr^{-1} in 1986–2002, 145 Mt yr^{-1} in 2003–2012 (following the construction of the Three Gorges Dam (TGD)), and finally 118 Mt yr^{-1} in 2013–2015 (following the construction of cascade dams) (Yang et al., 2018). Sediment loads discharged into the ECS decreased drastically after the impoundment of the TGD, even below the threshold value of the sediment loads transported from the Changjiang subaqueous delta (CSD) to the Zhe-Min coastal mud belt (ZMCMB) by the southward Zhe-Min coastal current (Fig. 1) (the threshold value is 150 Mt yr^{-1}, based on the deposition rate of the Holocene mud wedge in the ECS' inner shelf) (Xu et al., 2012; Yang et al., 2018). Therefore, sediments deposited into the CSD could be eroded and transported southward, which would change the sedimentary environment in the estuarine–inner shelf areas of the ECS (Gao et al., 2017; Wang et al., 2018). These variations will inevitably change the distribution, sources, and transport of OCPs in the estuarine–inner shelf regions of the ECS.

The above review shows that human-induced catchment changes are changing the system stability of the ECS, which could impact the fate of OCPs and further influence ecological safety in the ECS. Consequently, investigating the impacts of human activities on the source-to-sink transport of OCPs in the ECS is necessary and urgent. In the early 21st century, several ECS-related studies focused on the distribution, fate, and flux of OCPs (Yang et al., 2005; Hu et al., 2011; Lin et al., 2012), as well as their air–seawater exchange (Lin et al., 2015; Zhong et al., 2014; Li et al., 2017). Hu et al. (2011) suggested that the direct riverine inputs and shelf mud depositional process were dominant factors controlling the distribution and fate of the OCPs in the ECS. However, limited attention has been paid to the variations in OCPs in surface sediments considering the influence of human activities, which is valuable for understanding the regional OCP cycle. In this study, we examined the sediment grain size, total organic carbon (TOC), and OCPs in surface sediments from the estuarine–inner shelf areas of the ECS, and compared these values before and after the impoundment of the TGD. Our specific goals were to determine the changes in the levels and spatial patterns of the OCPs in the study area after the TGD impoundment. In particular, we wanted to explore how OCPs in the estuarine–inner shelf areas of the ECS respond to human-induced catchment changes.

2. Materials and methods

2.1. Sample collection

A total of 149 surficial sediment samples were collected from the estuarine–inner shelf areas of the ECS using a stainless steel box corer during three cruises conducted by R/V *Xiang Yang Hong* 18 and *Ke Xue* 3 in May 2018. The sampling sites distributed as highlighted in Fig. 1b. All samples (0–2 cm) were wrapped in aluminum foil and stored at −20 °C until the analysis.

2.2. Data acquisition

In this study, information on sediment grain size (n = 126), TOC content (n = 126), and OCP concentrations (n = 114) produced in 2006 was sourced from previous studies (Hu et al., 2011; Lin et al., 2012; Wang et al., 2017). All these samples were collected from the estuarine-inner shelf areas of the ECS in the summer of 2006 and 2007. Data on sedimentation rate before impoundment of the TGD (n = 76) were collected from Wang et al. (2017) and those on the sedimentation rate after impoundment (n = 76) were sourced from Gao et al. (2019). Two types of OCPs were studied in this work: HCHs (α-HCH, β-HCH, γ-HCH) and DDTs (p,p′-DDT, p,p′-DDE, p,p′-DDD).

2.3. Laboratory analysis

A standard mixed solution containing HCH (α-HCH, β-HCH, γ-HCH, δ-HCH) and DDT (p,p'-DDT; o,p'-DDT; p,p'-DDD and p,p'-DDE) was purchased from AccuStandard. All solvents (dichloromethane, acetone, and n-hexane) used during the processing were of HPLC grade. Analytical grade anhydrous sodium sulfate was activated at 450 °C for 5 h to remove impurities before use. Silica gel (100–200 mesh) was extracted using acetone, dichloromethane, and n-hexane for 24 h and activated for approximately 16 h at 130 °C.

OCP was extracted as per Lin et al. (2012). Each freeze-dried and homogenized sample (ca. 5 g) was Soxhlet-extracted using 100 mL of dichloromethane for 24 h and 2 g of activated copper was added for desulfurization. A mixture of TC*m*X and PCB209 was added to each of the samples as surrogate standards prior to extraction. The extracted solution was concentrated to 1–2 mL in a rotary evaporator and cleaned using a chromatography column (8 mm i. d.) with neutral alumina (3 cm, 3% deactivated), neutral silica gel (3 cm, 3% deactivated), 50% (on a weight basis) sulfuric acid silica (2 cm), and anhydrous sodium sulfate. The concentrated solution was added to the column and eluted with 20 mL of n-hexane/dichloromethane (1: 1 v/v). The eluate containing the OCPs was vacuum-evaporated and solvent-exchanged with n-hexane and finally concentrated to 1 mL under a gentle stream of nitrogen.

A Thermo Fisher Scientific TSQ 8000 Evo GC-MS/MS equipped with a fused silica capillary TG5-MS column (30 m × 0.25 mm internal diameter, 0.25 μm film thickness) was used to determine the concentration of the OCPs. Helium was used as the carrier gas with a flow rate of 1.0 mL min^{-1}. The GC temperature model was as follows: an initial temperature of 80 °C was maintained for 2 min

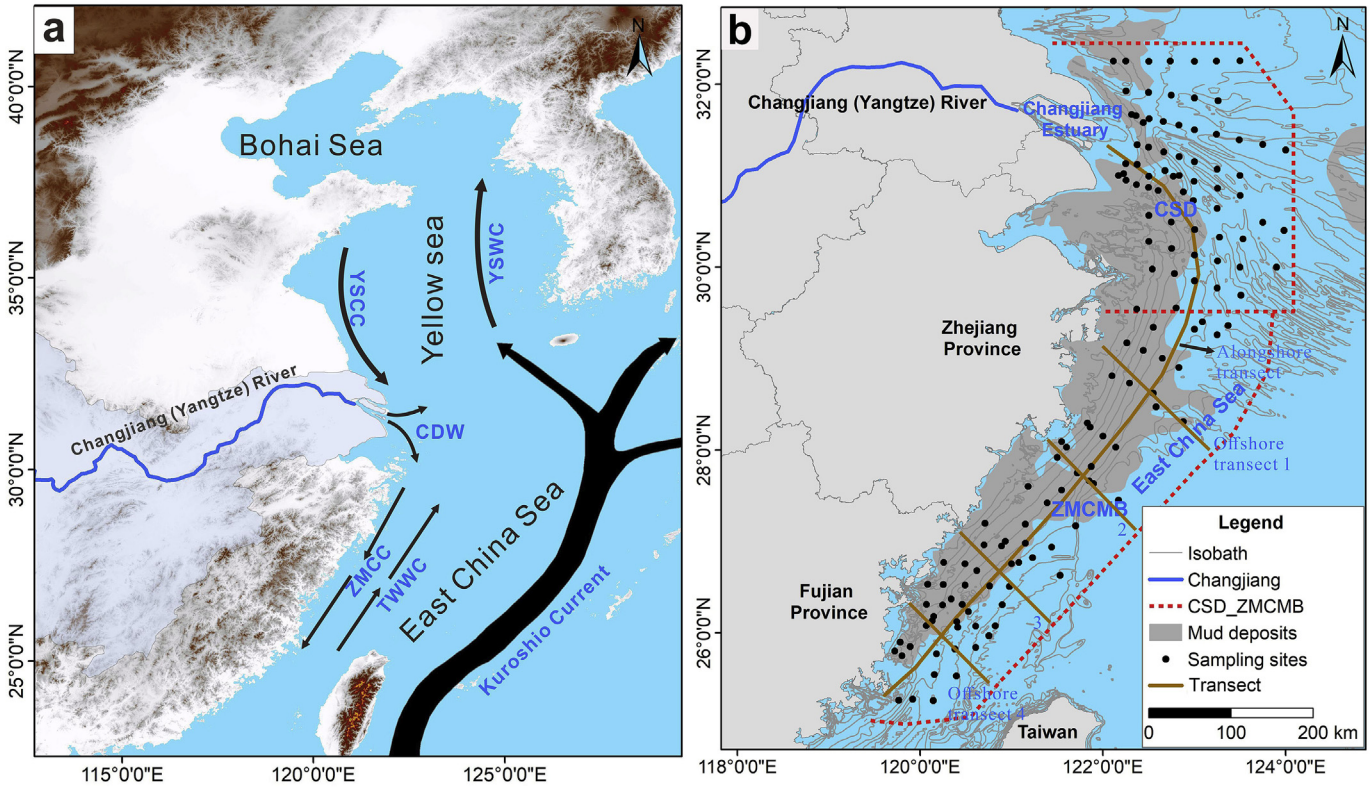

Fig. 1. Study area within the East China Sea showing (a) major oceanic currents including the Changjiang-diluted water (CDW), Zhe-Min coastal current (ZMCC), Taiwan warm current (TWWC), Yellow Sea coastal current (YSCC), Yellow Sea warm current (YSWC), and Kuroshio current; and (b) sampling sites along the Changjiang (Yangtze) River Estuary and inner shelf regions. The red dotted line represents the delineations of the Changjiang Subaqueous Delta (CSD) and the Zhe-Min Coastal Mud Belts (ZMCMB). (For interpretation of the references to colour in this figure legend, the reader is referred to the Web version of this article.)

and increased at a rate of 20 °C min^{-1} to 180 °C and held for 5 min. Then, it was increased at a rate of 10 °C min^{-1} to 290 °C and maintained for 15 min. The injection port was set at 290 °C. Subsequently, 1 μL of the sample extract was injected in the split-less mode. The interface and ion source temperatures were maintained at 290 and 230 °C, respectively. The ionization was carried out in the electron impact mode at 70 eV and data were acquired using the selective reaction monitoring mode.

A procedural blank and matrix-spiked samples consisting of all analytes were analyzed with each six-sample set. Duplicates were run for every 12 samples and the samples were reanalyzed if the difference exceeded more than 15%. The OCPs were quantified using the external standard method. Calibration curves were drawn based on the sets of six standard concentrations of 1, 10, 50, 100, 250, and 500 ng mL^{-1}. The standard curve was checked every day using the reference standard to ensure satisfactory linear regression coefficients ($R^2 > 0.999$) for all the OCPs tested. The p,p'-DDT was detected in some blank samples and its concentration ranged from 0 to 0.02 ng g^{-1}, with a mean value of 0.004 ± 0.002 ng g^{-1} ($n = 14$). This was 6.7% of the lowest observed concentration in our sediment samples, and therefore negligible. The average recoveries of the OCPs based on matrix-spiked samples ranged from 74.5% to 106.2%. The average surrogate recoveries were 68 ± 13% and 95 ± 9% for TC*m*X and PCB209, respectively.

The grain size was analyzed as described by Wang et al. (2018). Briefly, all samples were digested by an H_2O_2 solution (10%) to remove the organic matter and then dispersed in sodium metaphosphate for 24 h. The grain size was measured using a laser diffraction particle size analyzer (Mastersizer 2000; Malven Instruments Ltd., UK) and the measuring error was within 3%. Each freeze-dried and homogenized sediment was immersed in 10% hydrochloric acid for 24 h and washed to neutrality. The resulting material was wrapped in a silver boat to measure the TOC content using an elemental analyzer (Flash, 2000HT).

2.4. Kriging interpolation

The kriging interpolation method was used to acquire the spatial variability of each dataset using the same gridding density for the same areas in the ECS shelf regions. The most widely used geostatistical technology is the ordinary kriging interpolation, which uses linear, spatial, and interpolator-estimated data at unsampled locations using a linear weight function of adjacent data points (Guney et al., 2010).

$$Z(x_0) = \sum_{i=1}^{n} \lambda_i Z(x_i) \quad (1)$$

where $Z(x_0)$ is the estimated value of Z at point x_0, $Z(x_i)$ is the sampled value at point x_i, and λ_i is the weight placed on $Z(x_i)$. We used ArcGIS 10.0 software for the mapping and spatial analysis.

2.5. Deposition flux

The OCP deposition flux in surface sediments was estimated to assess the extent of contamination, which was calculated using several sediment properties and OCP concentration, as shown in equation (2).

$$F_{deposition} = 10^{10} A \times C_{OCPs} \times \rho \times \omega \quad (2)$$

where A is the area of a given region (km^2), C_{OCPs} is the measured sedimentary OCP concentrations (ng g^{-1}), ρ is the dry density of the sediment samples (g cm^{-3}), and ω is the sedimentation rate (cm yr^{-1}) mentioned in section 2.2, which was collected from Wang et al. (2017). The recommended value of 1.2 g cm^{-3} was selected for ρ (Liu et al., 2007). The kriging interpolation method was used to obtain the spatial distribution of ω based on the accurately collected sedimentation rates for the study area.

3. Results and discussion

3.1. Changes in physicochemical parameters of sediments in estuarine–inner shelf areas of the ECS

Previous studies have demonstrated that the sediments deposited in the estuarine–inner shelf areas of the ECS are likely to lag behind changes in the Changjiang (Yangtze) River catchment by about 3 years (Hu et al., 2012; Gao et al., 2017), implying that the sedimentary environment in the ECS cannot change immediately when the catchment is changed. Therefore, samples collected from the ECS in 2006 could reflect the sedimentary environment in the ECS around 2003 (The TGD was completed in 2003) and these samples could be considered as having just been or even not been affected by the TGD impoundment. Therefore, 2006 can be regarded as the beginning year when the TGD affected the sedimentary environment of the ECS. Then, sediment loads decreased drastically after the TGD impoundment, which significantly changed the transport of terrestrial materials from the Changjiang (Yangtze) River to the ECS (Gao et al., 2019). To better understand the variations in sediment grain size response to human-induced catchment changes, we compared the sediment grain size in the ECS for two different time nodes: before the TGD (sample collected in 2006) and after the TGD (sample collected in 2018).

Fig. 2 shows that the sediment grain size changed in the ECS, becoming increasingly coarse after the impoundment of the TGD. In 2006, the sediment grain size ranged from 2.5 to 7.3 Φ ($\Phi = -\log_2 D$, where D is the sediment grain size (mm)), with a mean value of 6.4 ± 1.2 Φ (mean = 6.4, SD = 1.2; all further results refer to this). Previous studies have demonstrated that the sediments in the ECS were relatively fine in 1982, with particle sizes ranging from 6.3 to 7.1 Φ (mean value is 6.7 ± 0.2 Φ) (Gao et al., 2019), which is relatively consistent with that in 2006. Therefore, the impoundment of TGD in 2003 did not impact the sedimentary environment of the ECS immediately. In 2018, the grain size of the surface sediments ranged from 0 to 7.4 Φ, with a mean value of 4.4 ± 2.1 Φ, which showed a drastic decrease. A previous study suggested that a value of 0.5 Φ could be chosen as the threshold for significant changes in grain size, thereby enabling us to filter out the seasonal and spring–neap tidal variations (mostly between 0.1 and 0.3 Φ in the study area) (Yang et al., 2018). A significant coarsening trend occurred after the impoundment of the TGD, with the mean grain size increasing from 6.4 to 4.4 Φ. In addition, surface sediment at a depth of 2 cm does not easily reflect seasonal variations because the deposition rate in the study area is lower than 2 cm yr^{-1} (Wang et al., 2017). Therefore, the temporal resolution of surface sediment in this study is about 1–2 years, from which short-term seasonal variation cannot be extracted. In addition, we also collected sediment load data of Changjiang (Yangtze) River before and after the impoundment of the TGD. The sediment loads were 305 ± 44 Mt yr^{-1} during 1992 and 2002 (ten years before the TGD), which decreased to 132 ± 36 Mt yr^{-1} during 2004 and 2014 (ten years after the TGD) (Fig. S1). The SD value of sediment loads indicated that the interannual variation in sediment loads of Changjiang (Yangtze) River before TGD is little, which also suggested that the sedimentary environment in the ECS should be relatively stable in this stage. After the impoundment of the TGD, the interannual variations in the sediment loads of Changjiang (Yangtze) River was little but persistent seabed erosion also occurred in the ECS due to the low sediment loads. Therefore, the variations in the sediment grain size of the ECS between 2006 and 2018 were caused by the cumulative effect of persistent erosion.

The distribution patterns of sediment grain size from north of 29°N, where we noted coarsening in the CSD after the impoundment of the TGD (Fig. 2a), were consistent with the results of Yang et al. (2018), which stated that the surface sediment in the CSD coarsening was evident after the TGD. In addition, sediment grain size between 29°N and 27°N showed coarsening to a certain extent (Fig. 2a), which is consistent with the results of Gao et al. (2019). Sediment components in the ECS in 2006 and 2018 were calculated and compared to explain this coarsening phenomenon. The content of the clay component decreased in the whole region, especially north of 27°N (Fig. S2). The content of the silt component increased in the ZMCMB and the western part of the CSD but decreased in the eastern part of the CSD (Fig. S2). However, the sand content slightly increased in the ZMCMB and the western part of the CSD but increased drastically in the eastern part of the CSD (Fig. S2). Therefore, the sedimentary environment in the CSD might have been disturbed and a large amount of fine-grained particles such as clay and fine silt may have been resuspended and transported southward. In addition, the sedimentary environment in the northern and middle parts of the ZMCMB (between 29°N and 27°N) might have been disturbed, albeit at a relatively lesser extent than that of the CSD. These variations changed the original sediment distribution pattern in the seabed, which may have influenced the distribution and fate of OCPs in the marine environment.

In addition to sediment grain size, we delineated the distribution of the TOC content in the ECS in 2006 and 2018, which was considered an important factor influencing the distribution of the OCPs (Hu et al., 2011; Jin et al., 2017). The TOC content in the ECS ranged from 0.17 to 0.84% in 2006, with a mean value of 0.56 ± 0.16% (Fig. 3a). And now the TOC content varied from 0.11 to 0.81% in 2018, with a mean value of 0.45 ± 0.18% (Fig. 3b). A clear boundary occurred at 29°N, with the high TOC content mainly occurring in the ZMCMB and the western part of the CSD. The TOC content evidently varied in the ZMCMB (Fig. 3b). The TOC content in sediments from the outer shelf of the estuary and the ZMCMB decreased drastically, which might be due to the reduction in fine-grained sediments. Large amounts of TOC associated with fine-grained sediments were transported southward to the ZMCMB and even to the outer shelf. Overall, the spatial pattern of the TOC content in the estuarine–inner shelf areas of the ECS changed after the TGD impoundment, which is consistent with the distribution pattern of sediment grain size.

3.2. Variations in OCPs in ECS between 2006 and 2018

The concentrations of the total OCP, DDT, and HCH in 2006 and 2018 are compared in Fig. 4. The total OCP concentration in 2006 ranged from 0.14 to 6.41 ng g^{-1}, with a mean value of 2.55 ± 1.51 ng g^{-1} (Fig. 4a). However, the total OCP concentration in 2018 ranged from 0.06 to 4.38 ng g^{-1}, with a mean value of 1.08 ± 0.84 ng g^{-1} (Fig. 4d). The HCH concentration in 2006 ranged from 0.03 to 1.96 ng g^{-1}, with a mean value of 0.42 ± 0.20 ng g^{-1}, and the corresponding value in 2018 ranged from 0 to 0.91 ng g^{-1}, with a mean value of 0.20 ± 0.17 ng g^{-1}. Similarly, the concentration of DDT in 2006 ranged from 0.08 to 5.66 ng g^{-1}, with an average value of 1.74 ± 1.04 ng g^{-1}. This concentration also decreased drastically in 2018 (ranging from 0 to 3.61 ng g^{-1}, with a mean value of 0.89 ± 0.69 ng g^{-1}). Similar to sediment grain size, the OCP concentrations in surface sediments should be a mixed concentration

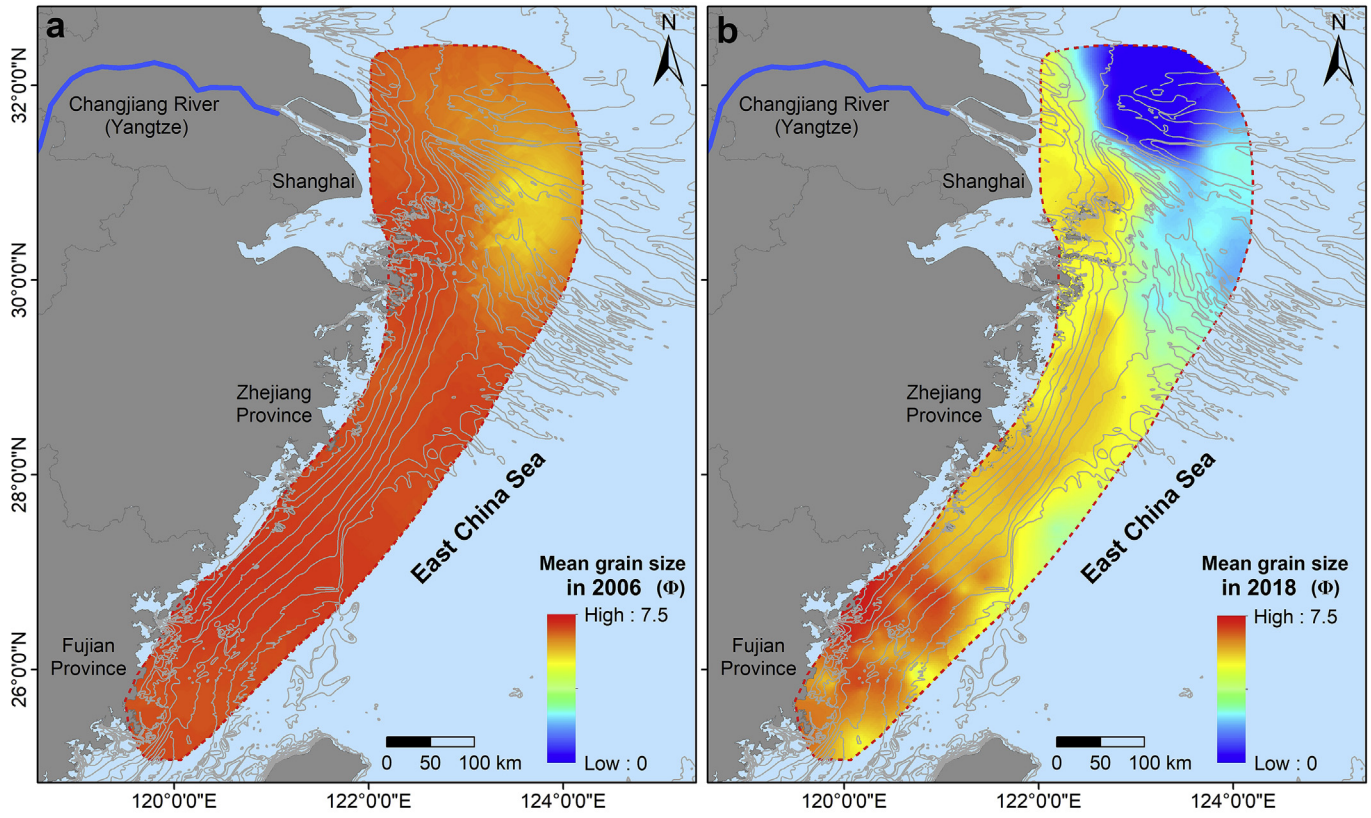

Fig. 2. Distribution patterns of surface sediment grain size from the estuarine–inner shelf areas of the ECS; (**a**) 2006, and (**b**) 2018.

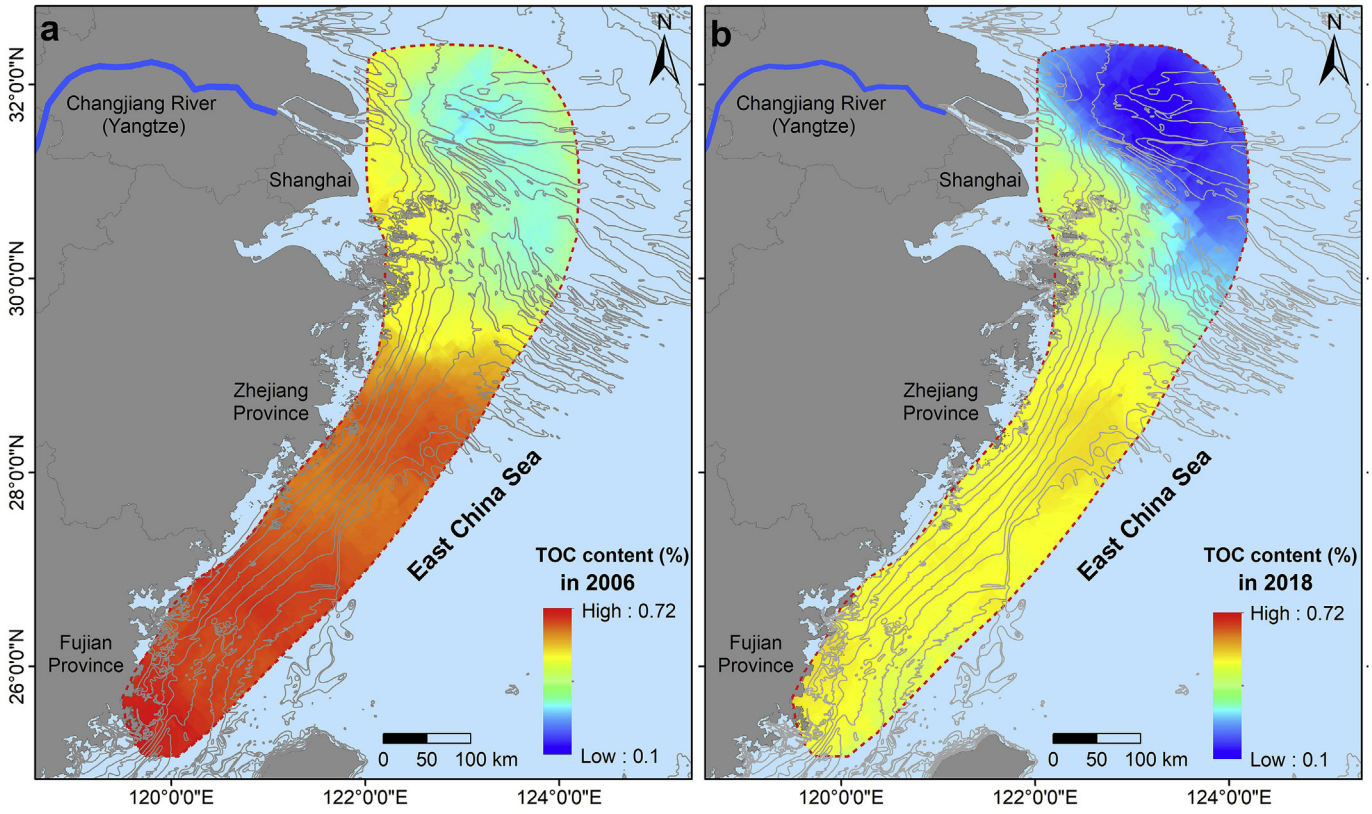

Fig. 3. Distribution patterns of TOC content in surface sediments from the estuarine–inner shelf regions of the ECS in 2006 (**a**) and 2018 (**b**).

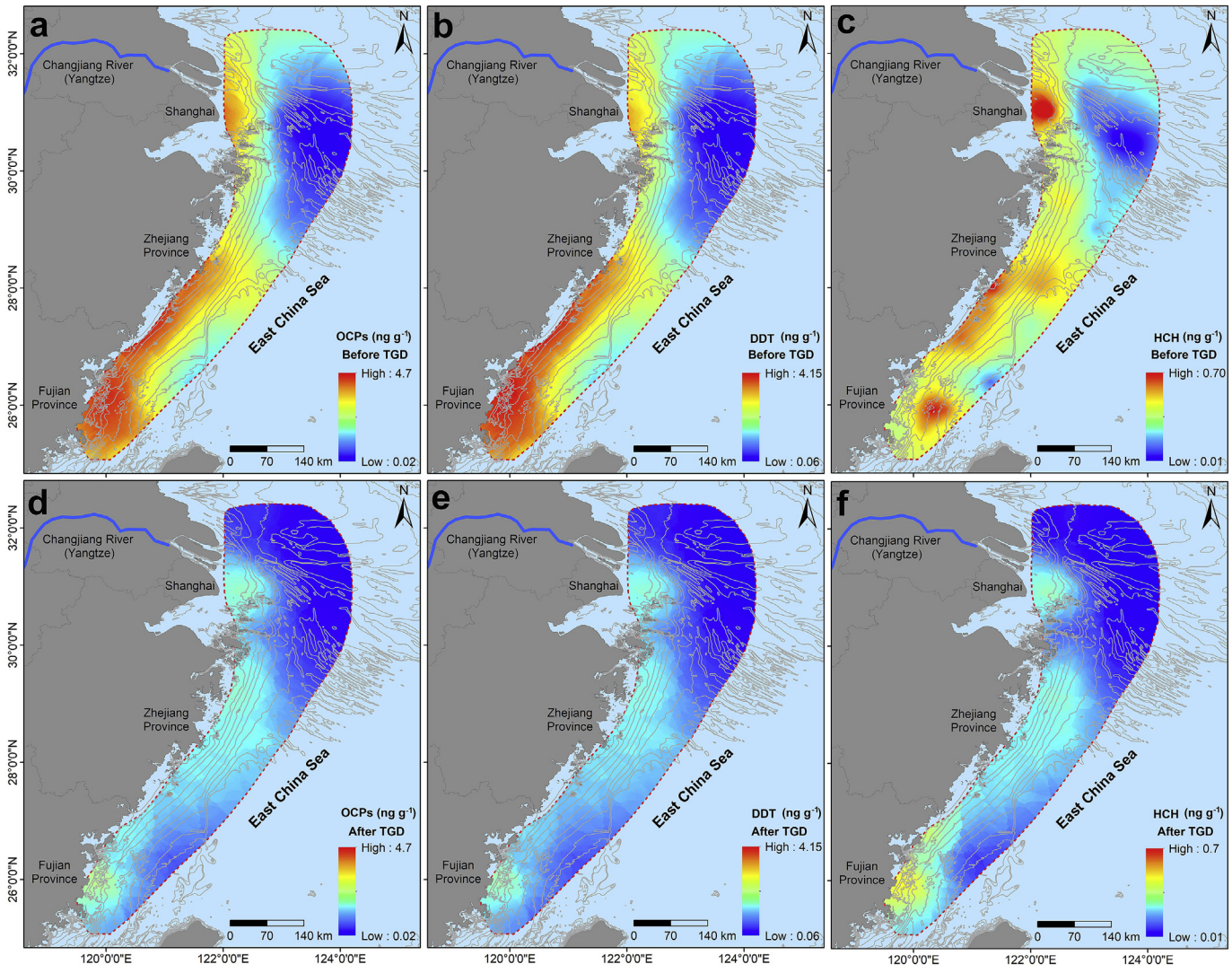

Fig. 4. Distribution patterns of OCPs, DDT, and HCH in surface sediments from the estuarine–inner shelf areas of the ECS in 2006 (upper row) and 2018 (lower row); (**a, d**) total OCP concentration, (**b, e**) DDT concentration, and (**c, f**) HCH concentration.

whose time scale should also be 1–2 years.

Considering spatial distribution, the total concentration of OCPs in the ECS showed an obvious difference in 2006 and 2018. The study area can be divided into the northern (CSD) and southern (ZMCMB) portions at 29°N, which is consistent with the distribution pattern of the TOC content (Fig. 3). High total OCP concentrations were found in the western part of the CSD and the ZMCMB (Fig. 4), which could be attributed to the terrestrial input and regional hydrodynamics (Hu et al., 2011). The Changjiang-Diluted Water (CDW) (Fig. 1a) discharges large amounts of sediments and associated OCPs into the estuary during the wet season (May to October), leading to a high total OCP concentration near the estuary. Then, in the dry winter season (November to April), the East Asian monsoon strengthens the southward current named the Zhe-Min coastal current (Fig. 1a), leading to the resuspension of the deposited sediments and associated OCPs into the estuary. They are transported southward and eventually deposited into the ZMCMB.

Fig. 4 also shows that high concentrations of total OCPs mainly occurred in nearshore areas, especially in 2006. To better understand the distribution patterns of OCPs in the study area, we utilized the ProfileGraph in ArcGIS 10.2 to extract OCP concentrations in five typical transects from the Changjiang Estuary to the southern part of the ZMCMB (Fig. 1b). OCPs in the alongshore transect from the estuary to the ZMCMB displayed high concentrations in the CSD and ZMCMB (Fig. 5a and b). OCPs in the offshore transects from the land to the ocean showed a consistent downward trend (Fig. 5c–j), suggesting that the total OCP concentration decreased from the coast to the ocean. Therefore, in addition to the effects of hydrodynamics, proximity to OCP sources should be the other main reason for the relatively high concentration of OCPs in the ZMCMB (Lin et al., 2012). Previous surveys have indicated that coastal provinces, including Zhejiang and Fujian, were major users of OCPs during 1985–1991, and their OCP consumption per unit area ranked first and third among all provinces in the country, respectively (Wang et al., 2005). Pesticide residues in the soil could therefore be entering the ECS via coastal mountain streams and surface runoff.

3.3. *Response of OCPs to changes in the river catchment*

After the impoundment of the TGD, the total OCP concentration in surface sediments from the estuarine–inner shelf areas of the ECS decreased drastically, which seems consistent with the timeline of the official ban of OCPs in China. Previous studies have

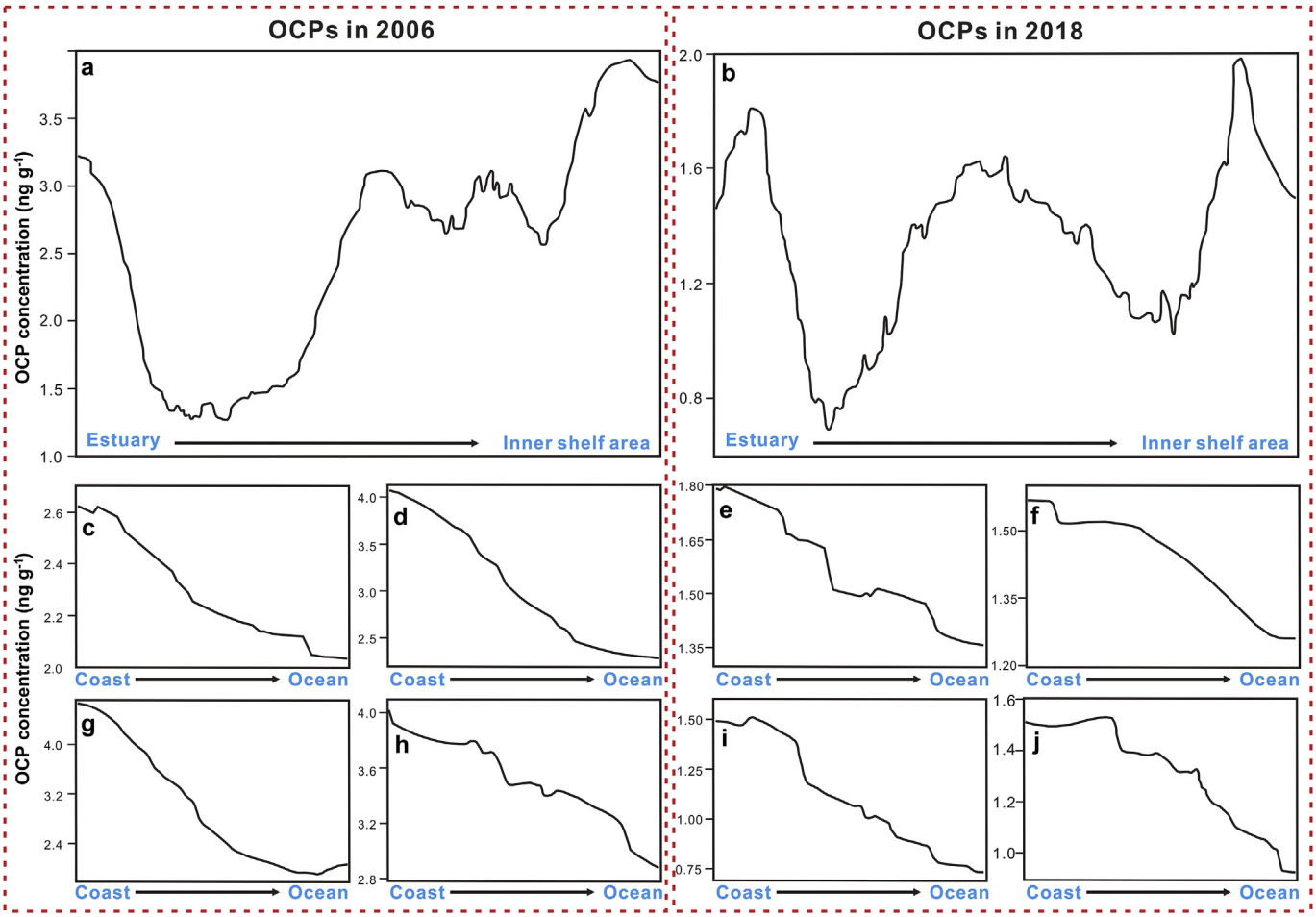

Fig. 5. Distribution of OCPs in alongshore and offshore transects from the estuarine–inner shelf areas of the ECS in 2006 (**left column**) and 2018 (**right column**); (**a**) alongshore transect in 2006, (**b**) alongshore transect in 2018, (**c, d, g, h**) offshore transects 1–4 in 2006, and (**e, f, i, j**) offshore transects 1–4 in 2018. (Note different scales on y-axis.)

demonstrated that OCPs in the air of the Arctic and East Asia showed a clear declining trend after their ban (Ma et al., 2011; Takazawa et al., 2016). Then, is the decrease in the total OCP concentration in the sediments due to the official ban? It is known that OCPs in the surface sediments of the ECS originated mainly from the continent due to soil erosion after their ban in China. Data on OCP concentrations in the topsoils of the Changjiang River Delta (CRD) before and after the TGD impoundment were collected in this study, and a clear decreasing trend was not observed; in fact, an increasing trend was noted after 2007 (Table 1). Sedimentary records of OCPs in inland lakes as well as the ECS also did not show a clear decreasing trend after the 2000s, suggesting that OCP concentrations in the soils of the river catchment did not decrease overall after the 2000s (Liu et al., 2009; Li et al., 2015; Lin et al., 2016; Sun et al., 2018). Zhang et al. (2018) demonstrated that the decline in DDT concentrations in the topsoil at the national scale was not obvious over time from 2001 to 2013 because the degradation of DDT in topsoil can take decades (Dimond and Owen, 1996; Zhang et al., 2018). In addition, these studies reported a new input of DDT, contained in the pesticide dicofol, to the soils of the CRD (Jiang et al., 2009; Sun et al., 2016). The new input and resistance to degradation could be the two main reasons for the absence of clear decrease in OCP concentrations in the soil of the Changjiang catchment. Therefore, the OCPs input from soil erosion into rivers did not change much, which strongly suggests that the drastic decrease in OCP concentrations in sediments from the ECS was not caused by the OCP ban.

In addition to the OCP concentration in topsoil, sediment loads

Table 1
OCP levels (ng g^{-1} d.w.) in the topsoils of Changjiang (Yangtze) River Delta (CRD) from different sampling years.

Region	Sampling year	N	range		mean		Reference
			t-HCH	t-DDT	t-HCH	t-DDT	
CRD	2003	161	0.28–17.93	0.46–484.24	3.23	28.87	Zhang et al. (2009)
CRD	2007	36	nd–10.38	0.44–247.45	2.41	21.41	Jiang et al. (2009)
CRD	2014	241	0.37–30.3	0.13–3515	2.46	56.2	Sun et al. (2016)
CRD	2014	19	0.69–66.69	0.14–485.73	7.73	44.43	Shi et al. (2016)

t-HCH = α-HCH + β-HCH + γ-HCH.
t-DDT = p,p′-DDT + p,p′-DDE + p,p′-DDD.

Table 2
Correlation coefficient (r) matrix of the OCPs and sediment features in the ECS.

	Before TGD (N = 95)*			After TGD (N = 149)		
	OCPs	DDT	HCH	OCPs	DDT	HCH
Mz**	0.58	0.59	0.37	0.75	0.74	0.74
Clay	0.35	0.36	0.20	0.46	0.43	0.55
Silt	0.58	0.58	0.39	0.78	0.78	0.74
Sand	−0.57	−0.58	−0.34	−0.77	−0.77	−0.76
TOC	0.62	0.64	0.38	0.85	0.85	0.81

Note: *N is number of sample; **Mz is mean grain size.

could be another factor impacting the OCP flux discharged into the ECS. Previous studies have demonstrated that the sediment loads discharged into the ECS decreased gradually since the 1980s and decreased drastically, from 340 Mt yr^{-1} in 1986–2002 to 145 Mt yr^{-1} in 2003–2012, after the impoundment of the TGD (Yang et al., 2018). Therefore, large amounts of OCPs adsorbed on the surface of the sediments were also intercepted in the reservoir, which led to the drastic decrease in the OCP flux discharged into the ECS. As mentioned above, there may not be a significant change in the OCPs content entering the river system through soil erosion, but the sediments load decreased by more than 57%, which might have also led to a substantial reduction in the OCP flux discharged into the ECS. Those OCPs discharged into the ECS are more widely dispersed and diluted, which might have directly caused the decrease in the OCP concentration in the surface sediments after the impoundment of the TGD.

It is well known that DDT and HCH are highly hydrophobic in nature. Thus, they have low water solubility and are prone to adsorption onto fine-grained particles such as clay and silt (Shen and Wania, 2005). Therefore, sediment loads discharged from the Changjiang (Yangtze) River into the ECS could play an important role in controlling the distribution patterns of OCPs in the ECS. Pearson Correlation analysis was carried out between the OCP concentrations and sediment grain size/components, and the results showed strong positive correlation between OCP concentration and grain size/silt component in 2006 and 2018 (Table 2). However, correlation between the OCP concentration and clay component was weak than that for the grain size or silt component (Table 2). This phenomenon may be controlled mainly by the composition ratios of clay and silt components because the clay content is limited while that of silt dominates (Fig. 2). A strong negative correlation is evident between the OCP concentration and the sand component (Table 2). Additionally, the absolute value of the correlation coefficient after the TGD impoundment increased to a certain extent, increasing by approximately 0.2 for each item except the clay component (Table 2). Therefore, the influence of sediment grain size on the distribution patterns of the OCPs might be more obvious after the impoundment of the TGD. Large amounts of sediments were intercepted by the reservoir, leading to "hungry" water discharge (i.e., water with a low suspended sediment concentration) and further enhancing the current's ability to carry sediment, eventually causing seabed erosion in the CSD and northern part of the ZMCMB (Fig. 2). Large amounts of fine particles, especially clay and fine silt components, could have been eroded and transported southward. Therefore, the clay component decreased, and the dominance of the silt component was further enhanced in the ECS, which may have been the main cause for the improvement in the r value.

3.4. Deposition flux of OCPs in the ECS in 2006 and 2018

To further understand the variations in the OCPs in 2006 and 2018, deposition fluxes of the OCPs were calculated for these two

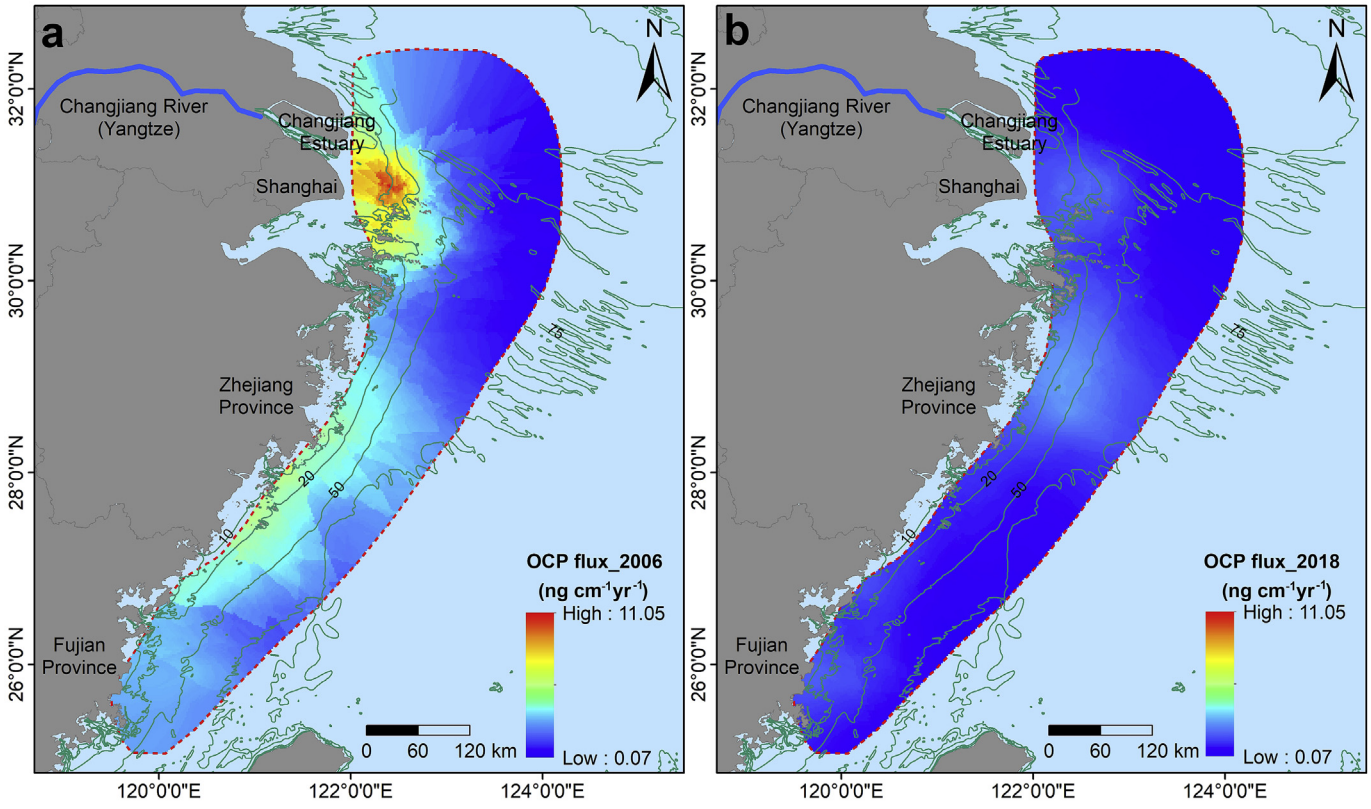

Fig. 6. Deposition fluxes of OCPs in the estuarine–inner shelf areas of the ECS in 2006 (**a**) and 2018 (**b**).

stages. The OCP deposition flux was calculated following the work by Lin et al. (2013) (as described briefly in Section 2), using the Map Algebra Technology of ArcGIS 10.2 software (Wang et al., 2017). The deposition fluxes of the OCPs in the ECS varied from 0.28 to 11.05 ng cm^{-2} yr^{-1}, with a mean value of 2.65 ± 1.67 ng cm^{-2} yr^{-1} in 2006 (Fig. 6a). After the impoundment, the sedimentation rate and OCP concentration in the ECS decreased, which also led to a reduction in the OCP deposition flux ranging from 0.07 to 2.60 ng cm^{-2} yr^{-1}, with a mean value of 0.89 ± 0.60 ng cm^{-2} yr^{-1} (Fig. 6b). Our previous study demonstrated that the deposition flux is determined by the deposition rate and compound concentration (Wang et al., 2016). The deposition rate and OCP concentration in the ECS decreased strongly after the TGD impoundment, thereby leading to a drastic decrease in the OCP flux. In addition, the distribution pattern of the OCP flux evidently changed after the TGD impoundment (Fig. 6). In summary, the OCPs in the sediments of

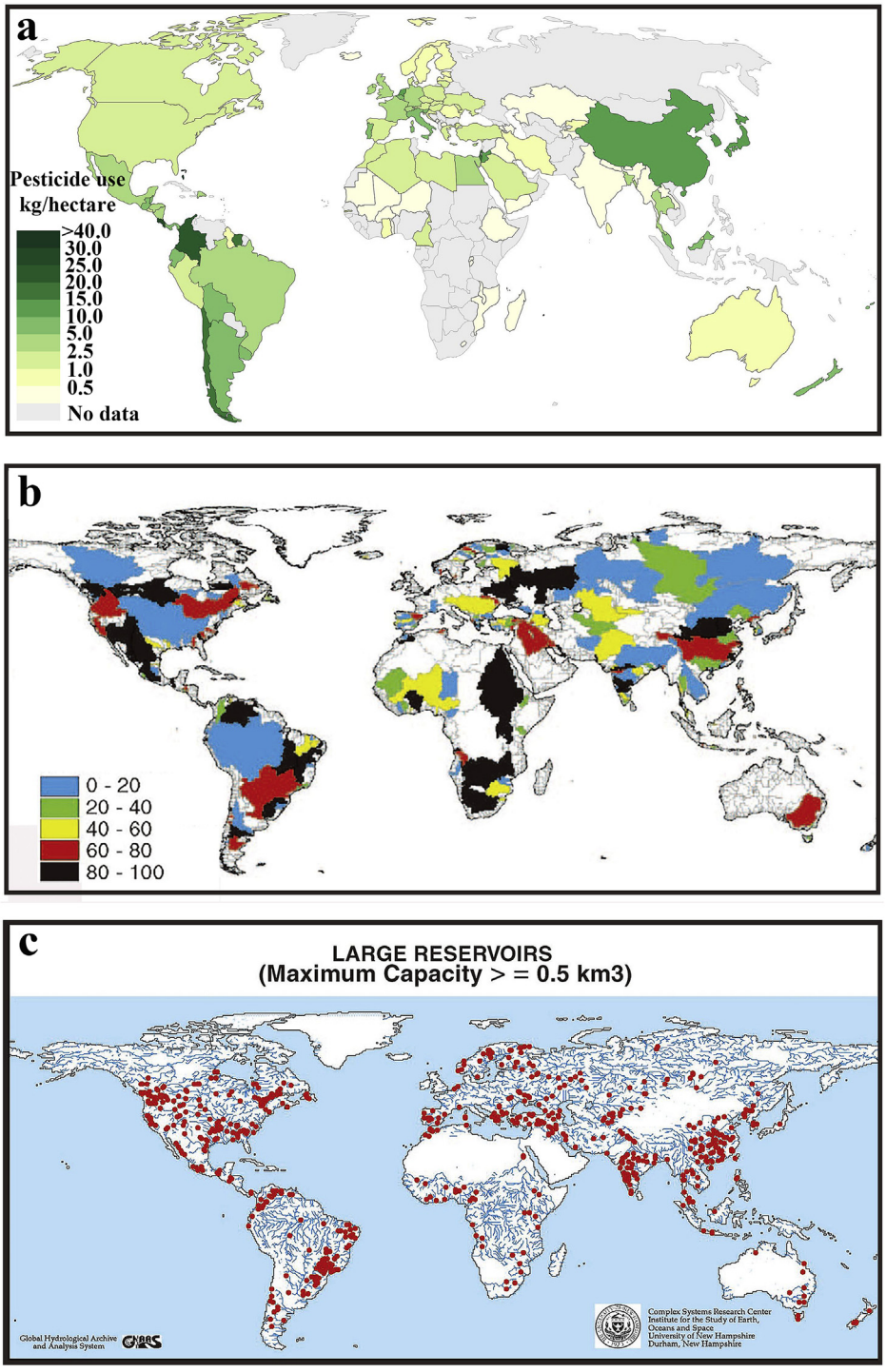

Fig. 7. Distribution patterns of pesticide use (https://ourworldindata.org/fertilizer-and-pesticides), large reservoirs (Vörösmarty et al., 2003), and sediment trapping efficiency (Vörösmarty et al., 2003) at the global scale. (**a**) Average pesticide use per hectare of cropland in 2007, measured in kilograms per hectare. (**b**) Global distribution of the 633 large reservoirs with a storage capacity of 0.5 km^3 or larger. (**c**) Global distribution of basin-wide trapping of sediment loads by the large reservoirs.

the ECS changed drastically due to intensified human activities in the river catchment, which was mainly reflected in the variations in their distributions, concentrations, and deposition fluxes.

4. Implications

Marginal seas, especially river-dominated estuarine coastal regions, are the major repositories of terrestrial materials in the ocean, with more than 95% of riverine sediments buried therein (Syvitski et al., 2005; Bianchi and Allison, 2009). These sediments include large buried amounts of hydrophobic organic contaminants such as OCPs. These regions are active interfaces between the land and ocean and are subject to the effects of human activities. Fig. 7 shows the global distribution patterns of pesticide use in cropland and large reservoirs, and their trapping efficiencies for major rivers. Pesticides are mainly used in the middle- and low-latitude regions of countries, especially in China, Central Europe, North Africa, and South America (Fig. 7a). Similarly, large rivers with high runoffs and sediment loads, such as the Amazon, Nile, Mekong, Ganges-Brahmaputra, Changjiang, Huanghe, and Pearl Rivers, are mainly located in the regions with high pesticide use. Agricultural activities and soil erosion led to large amounts of OCPs being released into rivers and eventually discharged into the adjacent marginal seas. Therefore, marginal seas in the middle and low latitudes have been important sinks of OCPs and are characterized by a high OCP burden. However, dams and reservoirs constructed in river catchments worldwide have led to large amounts of sediments being intercepted by the reservoirs (Fig. 7b and c). Moreover, OCP influxes via rivers have likely reduced owing to their hydrophobicity. Therefore, shifts in the distribution and fate of sedimentary OCPs in marginal seas under the influence of human activities is likely to be prevalent globally. It is noteworthy that owing to unique human-induced catchment changes in each marginal sea, the mode and extent of this influence will vary, resulting in differences in the fate of the OCPs.

5. Conclusions

This study comprehensively investigated the OCP distribution patterns and deposition flux in the ECS in 2006 and 2018. Human-induced catchment change is considered to be the main factor controlling the distribution and fate of OCPs in the ECS. The major conclusions of this study are as follows:

1 The OCP concentrations in the ECS in 2006 ranged from 0.14 to 6.41 ng g^{-1}, with a mean value of 2.55 ± 1.51 ng g^{-1}. The OCP concentrations clearly decreased in 2018, ranging from 0.01 to 4.38 ng g^{-1}, with a mean value of 1.08 ± 0.84 ng g^{-1}.
2 The deposition fluxes of OCPs in the ECS varied from 0.28 to 11.05 ng cm^{-2} yr^{-1}, with a mean value of 2.65 ± 1.67 ng cm^{-2} yr^{-1} in 2006. And then the sedimentation rate and OCP concentration in the ECS decreased in 2018, which also led to a reduction in the OCP deposition flux from 0.07 to 2.60 ng cm^{-2} yr^{-1}, with a mean value of 0.89 ± 0.60 ng cm^{-2} yr^{-1}.
3 The correlation analysis showed a good correlation between the OCP concentrations and the silt component. The r value increased by more than 0.2 after the TGD impoundment. Therefore, riverine input might have been the main factor controlling the fate of OCPs before the TGD impoundment, and seabed erosion owing to reduction in sediment loads might be the primary controlling factor after the impoundment.

Declaration of competing interest

The authors declare that they have no known competing financial interests or personal relationships that could have appeared to influence the work reported in this paper.

Acknowledgements

The study was supported by the Marine Science and Technology Innovation Project of Jiangsu Province (HY2018-9), the National Science Foundation of China (Grant nos. 41471431, 41601560, and 41776048), the Science Foundation for Youths of Jiangsu Province (BK20170438), and the Fundamental Research Funds for the Central Universities (Grant 14380001). We would like to thank Editage (www.editage.cn) for English language editing. The data for this study are provided in the supporting information.

Appendix A. Supplementary data

Supplementary data to this article can be found online at https://doi.org/10.1016/j.watres.2019.115225.

References

Ali, U., Syed, J.H., Junwen, L., Sánchezgarcía, L., Malik, R.N., Chaudhry, M.J., et al., 2014. Assessing the relationship and influence of black carbon on distribution status of organochlorines in the coastal sediments from Pakistan. Environ. Pollut. 190 (4), 82–90.
Alava, J.J., Cheung, W.W., Ross, P.S., Sumaila, R.U., 2017. Climate change-contaminant interactions in marine food webs: towards a conceptual framework. Glob. Chang. Biol. 23 (10), 3984–4001.
Bianchi, T.S., Allison, M.A., 2009. Large-river delta-front estuaries as natural "recorders" of global environmental change. Proc. Natl. Acad. Sci. 106 (20), 8085–8092.
Bigot, M., Hawker, D.W., Cropp, R., Dcg, M., Jensen, B., Bossi, R., et al., 2017. Spring melt and the redistribution of organochlorine pesticides in the sea-ice environment: a comparative study between Arctic and Antarctic regions. Environ. Sci. Technol. 51, 8944–8952.
Connor, M.S., Davis, J.A., Leatherbarrow, J., Greenfield, B.K., Gunther, A., Hardin, D., et al., 2007. The slow recovery of San Francisco Bay from the legacy of organochlorine pesticides. Environ. Res. 105 (1), 87–100.
Dimond, J.B., Owen, R.B., 1996. Long-term residue of DDT compounds in forest soils in Maine. Environ. Pollut. 92 (2), 227–230.
Gao, S., 2013. Holocene shelf-coastal sedimentary systems associated with the Changjiang River: an overview. Acta Oceanol. Sin. 32 (12), 4–12.
Gao, S., Collins, M.B., 2014. Holocene sedimentary systems on continental shelves. Mar. Geol. 352, 268–294.
Gao, J.H., Jia, J.J., Sheng, H., Yu, R., Li, G.C., Wang, Y.P., Yang, Y., Zhao, Y., Li, J., Bai, F., Xie, W.J., Wang, A., Zou, X.Q., Gao, S., 2017. Variations in the transport, distribution and budget of 210Pb in sediment over the estuarine and inner shelf areas of the East China Sea due to Changjiang catchment changes. J. Geophys. Res. Earth. 122 (1), 235–247.
Gao, J.H., Jia, J., Kettner, A.J., Xing, F., Wang, Y.P., Li, J., et al., 2018. Reservoir-induced changes to fluvial fluxes and their downstream impacts on sedimentary processes: the Changjiang (Yangtze) River, China. Quat. Int. 493, 187–197.
Gao, J., Shi, Y., Sheng, H., Kettner, A., Yang, Y., Jia, J., Wang, Y., Li, J., Bai, F., Zou, X., Gao, S., 2019. Rapid changes of the Changjiang (Yangtze) River and East China Sea source-to-sink conveying system in response to human induced catchment changes: a synthesis. Mar. Geol. 414, 1–17.
Greenfield, B.K., Melwani, A.R., Bay, S.M., 2015. A tiered assessment framework to evaluate human health risk of contaminated sediment. Integr. Environ. Asses. 11 (3), 459–473.
Guan, Y.F., Wang, J.Z., Ni, H.G., Zeng, E.Y., 2009. Organochlorine pesticides and polychlorinated biphenyls in riverine runoff of the Pearl River Delta, China: assessment of mass loading, input source and environmental fate. Environ. Pollut. 157 (2), 618–624.
Guney, M., Onay, T.T., Copty, N.K., 2010. Impact of overland traffic on heavy metal levels in highway dust and soils of Istanbul, Turkey. Environ. Monit. Assess. 164 (1), 101–110.
Hu, L.M., Lin, T., Shi, X.F., Yang, Z.S., Wang, H.J., Zhang, G., et al., 2011. The role of shelf mud depositional process and large river inputs on the fate of organochlorine pesticides in sediments of the Yellow and East China Seas. Geophys. Res. Lett. 38 (3), 246–258.
Hu, L., Shi, X., Yu, Z., Lin, T., Wang, H., Ma, D., 2012. Distribution of sedimentary organic matter in estuarine–inner shelf regions of the East China Sea: implications for hydrodynamic forces and anthropogenic impact. Mar. Chem. 142–144, 29–40.
Jiang, Y.F., Wang, X.T., Jia, Y., Wang, F., Wu, M.H., Sheng, G.Y., et al., 2009. Occurrence, distribution and possible sources of organochlorine pesticides in agricultural soil of Shanghai, China. J. Hazard Mater. 170 (2–3), 989–997.
Jin, M., Fu, J., Xue, B., Zhou, S., Zhang, L., Li, A., 2017. Distribution and enantiomeric

profiles of organochlorine pesticides in surface sediments from the Bering Sea, Chukchi Sea and adjacent arctic areas. Environ. Pollut. 222, 109–117.
Lewis, S.L., Maslin, M.A., 2015. Defining the Anthropocene. Nature 519 (7542), 171–180.
Lewalle, A., Pepper, M., Ford, C.J.B., Hwang, E.H., Sarma, S.D., Paul, D.J., et al., 2009. Organochlorine pesticides and PAHs in the surface water and atmosphere of the north Atlantic and Arctic Ocean. Environ. Sci. Technol. 43 (15), 5633–5639.
Li, Y.F., Macdonald, R.W., 2005. Sources and pathways of selected organochlorine pesticides to the Arctic and the effect of pathway divergence on HCH trends in biota: a review. Sci. Total Environ. 342 (1), 87–106.
Li, C.C., Huo, S.L., Xi, B.D., Yu, Z.Q., Zeng, X.Y., Zhang, J.T., et al., 2015. Historical deposition behaviors of organochlorine pesticides (OCPs) in the sediments of a shallow eutrophic lake in Eastern China: roles of the sources and sedimentological conditions. Ecol. Indicat. 53, 1–10.
Li, Z., Lin, T., Li, Y., Jiang, Y., Guo, Z., 2017. Atmospheric deposition and air-sea gas exchange fluxes of DDT and HCH in the Yangtze River Estuary, East China Sea. J. Geophys. Res. Atmos. 122 (7), 7664–7677.
Lin, T., Hu, L., Shi, X., Li, Y., Guo, Z., Zhang, G., 2012. Distribution and sources of organochlorine pesticides in sediments of the coastal East China Sea. Mar. Pollut. Bull. 64 (8), 1549–1555.
Lin, T., Hu, L., Guo, Z., Zhang, G., Yang, Z., 2013. Deposition fluxes and fate of polycyclic aromatic hydrocarbons in the Yangtze River estuarine-inner shelf in the East China Sea. Glob. Biogeochem. Cycles 27 (1), 77–87.
Lin, T., Guo, Z., Li, Y., Nizzetto, L., Ma, C., Chen, Y., 2015. Air-seawater exchange of organochlorine pesticides along the sediment plume of a large contaminated river. Environ. Sci. Technol. 49 (9), 5354–5362.
Lin, T., Nizzetto, L., Guo, Z., Li, Y., Li, J., Zhang, G., 2016. DDTs and HCHs in sediment cores from the coastal East China Sea. Sci. Total Environ. 539, 388–394.
Liu, G., Zhang, G., Jin, Z., Li, J., 2009. Sedimentary record of hydrophobic organic compounds in relation to regional economic development: a study of Taihu lake, East China. Environ. Pollut. 157 (11), 2994–3000.
Liu, J.P., Xu, K.H., Li, A.E.A., Milliman, J.D., Velozzi, D.M., Xiao, S.B., Yang, Z.S., 2007. Flux and fate of yangtze river sediment delivered to the east China sea. Geomorphology 85 (3), 208–224.
Ma, J., Hung, H., Tian, C., Kallenborn, R., 2011. Revolatilization of persistent organic pollutants in the Arctic induced by climate change. Nat. Clim. Chang. 1 (5), 255.
Milliman, J.D., Farnsworth, K.L., 2013. River Discharge to the Coastal Ocean: a Global Synthesis. Cambridge University Press.
Shen, L., Wania, F., 2005. Compilation, evaluation, and selection of physical–chemical property data for organochlorine pesticides. J. Chem. Eng. Data 50 (3), 742–768.
Shi, L., Sun, Y.Y., Lu, A.J., Cai, X.H., Shen, X.M., Shen, J.L., 2016. Distribution characteristics of 22 organochlorine pesticides in soils from some areas of the Yangtze River Delta. Rock Miner. Anal. 35 (1), 75–81 ([In Chinese with English abstract]).
Steffen, W., Crutzen, P.J., Mcneill, J.R., 2007. The Anthropocene: are humans now overwhelming the great forces of nature? Ambio 36 (8), 614–621.
Sun, J., Pan, L., Zhan, Y., Lu, H., Zhu, L., 2016. Contamination of phthalate esters, organochlorine pesticides and polybrominated diphenyl ethers in agricultural soils from the Yangtze River Delta of China. Sci. Total Environ. 544, 670–676.
Sun, Y., Yuan, G.L., Li, J., Tang, J., Wang, G.H., 2018. High-resolution sedimentary records of some organochlorine pesticides in Yamzho Yumco Lake of the Tibetan Plateau: concentration and composition. Sci. Total Environ. 615, 469–475.
Syvitski, J.P.M., Vorosmarty, C.J., Kettner, A.J., Green, P., 2005. Impact of humans on the flux of terrestrial sediment to the global coastal ocean. Science 308, 376–380.
Takazawa, Y., Takasuga, T., Doi, K., Saito, M., Shibata, Y., 2016. Recent decline of DDTs among several organochlorine pesticides in background air in East Asia. Environ. Pollut. 217, 134–142.
Vörösmarty, C.J., Meybeck, M., Balázs, F., Sharma, K., Syvitski, J.P.M., 2003. Anthropogenic sediment retention: major global impact from registered river impoundments. Glob. Planet. Chang. 39 (1–2), 169–190.
Wang, T., Lu, Y., Zhang, H., Shi, Y., 2005. Contamination of persistent organic pollutants (POPs) and relevant management in China. Environ. Int. 31 (6), 0–821.
Wang, C., Zou, X., Gao, J., et al., 2016. Pollution status of polycyclic aromatic hydrocarbons in surface sediments from the Yangtze River Estuary and its adjacent coastal zone. Chemosphere 162, 80–90.
Wang, C., Zou, X., Zhao, Y., Li, Y., Song, Q., Wang, T., et al., 2017. Distribution pattern and mass budget of sedimentary polycyclic aromatic hydrocarbons in shelf areas of the Eastern China Marginal Seas. J. Geophys. Res. Oceans 122 (6), 4990–5004.
Wang, C., Zou, X., Feng, Z., Hao, Z., Gao, J., 2018. Distribution and transport of heavy metals in estuarine–inner shelf regions of the East China Sea. Sci. Total Environ. 644, 298–305.
Wong, F., Kurtkarakus, P., Bidleman, T.F., 2012. Fate of brominated flame retardants and organochlorine pesticides in urban soil: volatility and degradation. Environ. Sci. Technol. 46 (5), 2668–2674.
Xu, K., Li, A., Liu, J.P., Milliman, J.D., Yang, Z., Liu, C.S., Kao, S.J., Wan, S.M., Xu, F., 2012. Provenance, structure, and formation of the mud wedge along inner continental shelf of the East China Sea: a synthesis of the Yangtze dispersal system. Mar. Geol. 291, 176–191.
Yang, R.Q., Jiang, G.B., Zhou, Q.F., Yuan, C.G., Shi, J.B., 2005. Occurrence and distribution of organochlorine pesticides (HCH and DDT) in sediments collected from East China Sea. Environ. Int. 31 (6), 799–804.
Yang, H.F., Yang, S.L., Meng, Y., Xu, K.H., Luo, X.X., Wu, C.S., et al., 2018. Recent coarsening of sediments on the southern Yangtze subaqueous delta front: a response to river damming. Cont. Shelf Res. 155, 45–51.
Yang, S.L., Milliman, J.D., Li, P., Xu, K., 2011. 50,000 dams later: erosion of the Yangtze River and its delta. Glob. Planet. Chang. 75 (1–2), 1–20.
Zhang, G., Parker, A., House, A., Mai, B., Li, X., Kang, Y., et al., 2002. Sedimentary records of DDT and HCH in the Pearl River delta, South China. Environ. Sci. Technol. 36 (17), 3671–3677.
Zhang, H., Luo, Y., Li, Q., 2009. Burden and depth distribution of organochlorine pesticides in the soil profiles of Yangtze River Delta region, China: implication for sources and vertical transportation. Geoderma 153 (1–2), 0–75.
Zhang, C., Liu, L., Ma, Y., Li, F., 2018. Using isomeric and metabolic ratios of DDT to identify the sources and fate of DDT in Chinese agricultural topsoil. Environ. Sci. Technol. 52 (4), 1990–1996.
Zhong, G., Tang, J., Xie, Z., Möller, A., Zhao, Z., Sturm, R., Chen, Y., Tian, C., Pan, X., Qin, W., Zhang, G., Ebinghaus, R., 2014. Selected current-use and historicuse pesticides in air and seawater of the Bohai and Yellow Seas, China. J. Geophys. Res. Atmos. 119, 1073–1086.